

# Power Flow Solution for Multiphase Unbalanced Distribution Networks with High Penetration of Photovoltaics

Hossein Hooshyar, and Luigi Vanfretti

KTH Royal Institute of Technology, Stockholm, Sweden  
 hossein.hooshyar@ee.kth.se, luigi.vanfretti@ee.kth.se

## Abstract

**Power flow analysis on a Photovoltaic System (PV)-dominated distribution network is rather different than a conventional distribution system. This paper proposes a new three-phase power flow solution for such networks that considers the multiphase unbalanced nature of distribution systems together with different system topologies. Power flow contributions of PVs and different types of loads are also considered. The performance of the proposed method has been assessed by simulations on a sample distribution network.**

## 1. Introduction

Power flow is one of the main analyses performed in the process of planning, design, and operation of any power system. Traditional methods such as Gauss-Seidel and Newton-Raphson techniques perform power flow analysis assuming that the system is perfectly balanced. Due to the unbalanced multiphase nature of distribution systems, these methods fail to meet performance and accuracy requirements [1]. Also, traditional power flow methods consider loads as constant power demands. This assumption is not valid in distribution systems due to uncontrolled bus voltages as well as the constant current or constant impedance nature of some industrial and residential loads [2]. Traditional methods are not suitable when considering Distributed Generation (DG) such as Photovoltaic (PV) systems. The PVs, especially at the residential level, are single-phase power sources connected at different phases and therefore cannot be analyzed with traditional power flow methods, as they assume balanced operation [3].

A few methods for power flow analysis of such distribution systems have been proposed in the literature [2,4-9]. However, the majority of the proposed methods suffer from several drawbacks such as inability to consider non-radial networks and/or single-phase generators. This paper proposes a comprehensive power flow solution for PV-dominated distribution systems. The method considers multiphase unbalanced systems as well as different system topologies. The method also considers power flow contributions of single-phase PVs and different types of loads.

## 2. Models of components

### 2.1. PV system

To analyze the effects of PVs on the power flow, we need a model for the PV system first.

Fig. 1 shows a typical grid connected residential PV system. It is an inverter interfaced system to accommodate 120 Volt or 240 Volt AC connections [3].

The current to be injected from a PV to the system depends on the PV inverter design. Since the PV systems are designed to push the maximum power available from PV panels to the system, the PV inverter tries to push this power under any voltage condition, i.e., it will try to act like a constant power source. Hence, the current injection from a PV inverter to the system can be approximated as  $I = (P_{PV})/V$  where  $P_{PV}$  is the power from the PV panels and  $V$  is the AC terminal voltage. However, if this current gets to be higher than the maximum current rating of the inverter, inverter limits the current at its maximum level. Inverters limit their current to 1 to 2 times the rated current [10]. Thus, the PV system will have the V-I characteristics shown in Fig. 2 [11]. As indicated in the figure, the inverter current and voltage are usually in phase for unity power factor operation.

Here, the V-I characteristics shown in Fig. 2, introduced by [11], is used to estimate the current injection from a PV inverter to the system. This can be achieved by modeling the PV system as a controlled current source whose magnitude depends on its terminal voltage and PV panel power. Fig. 3 illustrates this model. Note that this model is for a typical voltage sourced based inverters used for grid connected PV systems. If the inverter is set to operate in a different control mode – for example for constant power factor mode – then the model needs to be revised accordingly.

This model will be used in the next section to consider the PVs contributions to power flows.

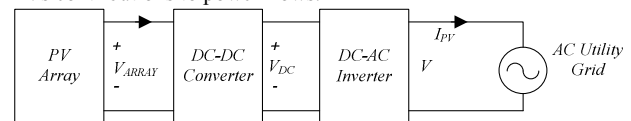


Fig. 1. Main components of a residential PV system.

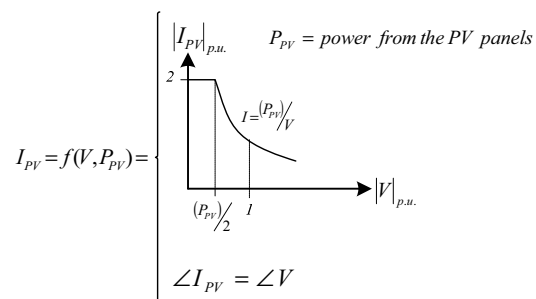


Fig. 2. V-I characteristics of a PV System.

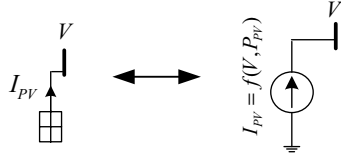


Fig. 3. PV model for system studies.

## 2.2. Loads

Fig. 4 shows the load models depending on the load characteristics. As shown in the figure, the constant current and the constant power loads are modeled with current sources whereas the constant impedance load is modeled with a resistor and an inductor. These models will be used in the next section to consider different types of loads in the power flow solution.

## 3. Power flow solution

### 3.1. Basic formulation

Fig. 5 shows a generic three phase line section with PVs and different types of loads connected at both ends.

The voltage drop across the phase 'a' of the line section can be determined as:

$$V_s^a - V_r^a = Z_{sr}^{aa} I_{sr}^a + Z_{sr}^{ab} I_{sr}^b + Z_{sr}^{ac} I_{sr}^c. \quad (1)$$

On the other hand,  $V_s^a$  and  $V_r^a$ , the terminal voltages of  $Z_{sCI}^a$  and  $Z_{rCI}^a$ , can be obtained from the following equations:

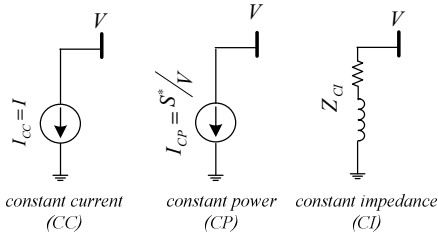


Fig. 4. Models for different types of loads.

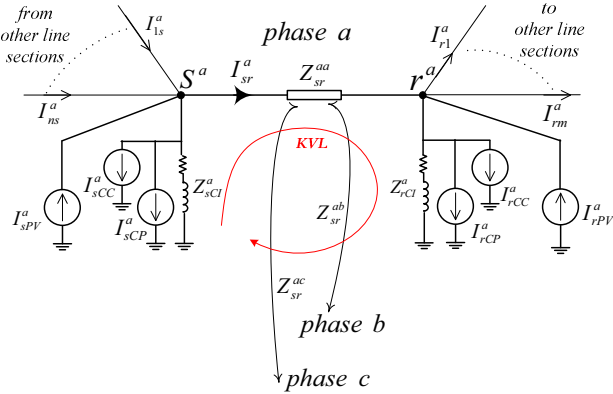


Fig. 5. A generic three phase line section with PVs and different types of loads connected at both ends.

$$V_s^a = Z_{sCI}^a \left( \sum_{i=1}^n I_{is}^a + I_{sPV}^a - I_{sr}^a - I_{sCC}^a - I_{sCP}^a \right). \quad (2)$$

$$V_r^a = Z_{rCI}^a \left( I_{sr}^a + I_{rPV}^a - \sum_{i=1}^m I_{ri}^a - I_{rCC}^a - I_{rCP}^a \right). \quad (3)$$

Now by replacing  $V_s^a$  and  $V_r^a$  in (1) by (2) and (3), we get to the following equation:

$$\begin{aligned} & -Z_{sCI}^a \sum_{i=1}^n I_{is}^a + (Z_{sCI}^a + Z_{sr}^{aa} + Z_{rCI}^a) I_{sr}^a - Z_{rCI}^a \sum_{i=1}^m I_{ri}^a + Z_{sr}^{ab} I_{sr}^b + Z_{sr}^{ac} I_{sr}^c \\ & = Z_{sCI}^a (I_{sPV}^a - I_{sCC}^a - I_{sCP}^a) - Z_{rCI}^a (I_{rPV}^a - I_{rCC}^a - I_{rCP}^a). \end{aligned} \quad (4)$$

Following the same logic, (5) and (6) give the same relation for phases 'b' and 'c', respectively.

$$\begin{aligned} & -Z_{sCI}^b \sum_{i=1}^n I_{is}^b + (Z_{sCI}^b + Z_{sr}^{bb} + Z_{rCI}^b) I_{sr}^b - Z_{rCI}^b \sum_{i=1}^m I_{ri}^b + Z_{sr}^{ab} I_{sr}^a + Z_{sr}^{bc} I_{sr}^c \\ & = Z_{sCI}^b (I_{sPV}^b - I_{sCC}^b - I_{sCP}^b) - Z_{rCI}^b (I_{rPV}^b - I_{rCC}^b - I_{rCP}^b). \end{aligned} \quad (5)$$

$$\begin{aligned} & -Z_{sCI}^c \sum_{i=1}^n I_{is}^c + (Z_{sCI}^c + Z_{sr}^{cc} + Z_{rCI}^c) I_{sr}^c - Z_{rCI}^c \sum_{i=1}^m I_{ri}^c + Z_{sr}^{ac} I_{sr}^a + Z_{sr}^{bc} I_{sr}^b \\ & = Z_{sCI}^c (I_{sPV}^c - I_{sCC}^c - I_{sCP}^c) - Z_{rCI}^c (I_{rPV}^c - I_{rCC}^c - I_{rCP}^c). \end{aligned} \quad (6)$$

Note that the unknown variables in (4) to (6) are the line currents,  $I_{sr}^a$ ,  $I_{sr}^b$ ,  $I_{sr}^c$ . As indicated in the equations, the contributions of PVs, constant power loads, and constant current loads in the power flow are considered by current sources whereas those of the constant impedance loads are considered by impedances. The currents of PVs and constant power loads are determined by the models introduced in the previous section assuming that the terminal voltages,  $V$ , are known.

Also, note that the currents directions can be determined arbitrarily. In this study, the directions of currents are assumed to be from the nodes with the lower numbers to the nodes with the higher numbers.

Deriving the same type of equations, for all line sections of a distribution system with  $N$  lines, results in a system of  $3N$  linear equations with  $3N$  variables. These equations will be used in the next part to form the system matrices.

### 3.2. Formulation of system matrices

The equations derived in the previous part are put into matrix form as expressed in (7). Note that in this equation, the state variables are the currents of the line sections.

$$[Zbus][Iline] = [ZI]. \quad (7)$$

where, for a system with  $N$  line sections,  $[Zbus]$  is a symmetric  $3N \times 3N$  matrix containing the system impedances,  $[Iline]$  is a  $3N \times 1$  matrix containing the line section currents as the system state variables, and  $[ZI]$  is a  $3N \times 1$  matrix containing the information of the loads and PVs connected to the line sections. Fig. 6 illustrates the structures of the matrices.

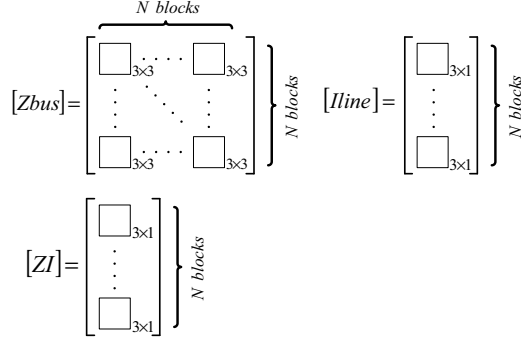


**Fig. 6.** Structures of the system matrices for the proposed power flow solution.

The line sections can be numbered in an arbitrary order. A building algorithm for these matrices can be developed as follows:

- $[Zbus]$ : As shown in Fig. 6,  $[Zbus]$  consists of  $N$  blocks of rows and  $N$  blocks of columns. The blocks are  $3 \times 3$  matrices. Each diagonal block belongs to a line section and shall be constructed according to (8). If the  $i^{th}$  and the  $j^{th}$  line sections are interconnected, the corresponding non-diagonal blocks shall be constructed according to (9); otherwise the  $(i, j)^{th}$  and the  $(j, i)^{th}$  blocks are null matrices.

$$[Zbus]_{(i,i)} = \begin{bmatrix} Z_{sCl}^a + Z_{sr}^{aa} + Z_{rCl}^a & Z_{sr}^{ab} & Z_{sr}^{ac} \\ Z_{sr}^{ab} & Z_{sCl}^b + Z_{sr}^{bb} + Z_{rCl}^b & Z_{sr}^{bc} \\ Z_{sr}^{ac} & Z_{sr}^{bc} & Z_{sCl}^c + Z_{sr}^{cc} + Z_{rCl}^c \end{bmatrix} \quad (8)$$

$$[Zbus]_{(i,j)} = [Zbus]_{(j,i)} = \begin{bmatrix} \pm Z_{Cl-between i^{th} and j^{th}}^a & 0 & 0 \\ 0 & \pm Z_{Cl-between i^{th} and j^{th}}^b & 0 \\ 0 & 0 & \pm Z_{Cl-between i^{th} and j^{th}}^c \end{bmatrix} \quad (9)$$

Note that the matrix entries in (9) are the constant impedance loads hooked up to the common node of the  $i^{th}$  and the  $j^{th}$  line sections. The ‘ $\pm$ ’ sign is ‘+’ if the line sections are interconnected via sending or receiving sides at the common node; otherwise, i.e. one side is sending and the other side is receiving, it’s ‘-’.

If the line section is single-phase or double-phase, the self and mutual impedances of the missing phase(s) are set to an extreme and zero, respectively. Also, the  $Z_{Cl}$  entries are set to an extreme if the corresponding loads do not exist. For example, equations 10 and 11 show the diagonal blocks for a single-‘a’-phase and a double-‘ab’-phase line section, respectively.

$$[Zbus]_{(i,i)} = \begin{bmatrix} Z_{sCl}^a + Z_{sr}^{aa} + Z_{rCl}^a & 0 & 0 \\ 0 & 1e10 & 0 \\ 0 & 0 & 1e10 \end{bmatrix} \quad (10)$$

$$[Zbus]_{(i,i)} = \begin{bmatrix} Z_{sCl}^a + Z_{sr}^{aa} + Z_{rCl}^a & Z_{sr}^{ab} & 0 \\ Z_{sr}^{ab} & Z_{sCl}^b + Z_{sr}^{bb} + Z_{rCl}^b & 0 \\ 0 & 0 & 1e10 \end{bmatrix} \quad (11)$$

Finally note that the building algorithm of  $[Zbus]$  is not based on the system topology, therefore the method can be used for both radial and meshed distribution systems.

- $[Iline]$ :  $[Iline]$  is a vector of  $N$   $3 \times 1$  blocks as shown in Fig. 6. Each block contains the three-phase currents of a line section as indicated in (12).

$$[Iline]_{(i)} = \begin{bmatrix} I_{sr}^a \\ I_{sr}^b \\ I_{sr}^c \end{bmatrix} \quad (12)$$

- $[ZI]$ : As shown in Fig. 6,  $[ZI]$  is a vector of  $N$   $3 \times 1$  blocks each containing the information of the loads and PVs connected to a line section as indicated in (13).

$$[ZI]_{(i)} = \begin{bmatrix} Z_{sCl}^a (I_{sPV}^a - I_{sCC}^a - I_{sCP}^a) - Z_{rCl}^a (I_{rPV}^a - I_{rCC}^a - I_{rCP}^a) \\ Z_{sCl}^b (I_{sPV}^b - I_{sCC}^b - I_{sCP}^b) - Z_{rCl}^b (I_{rPV}^b - I_{rCC}^b - I_{rCP}^b) \\ Z_{sCl}^c (I_{sPV}^c - I_{sCC}^c - I_{sCP}^c) - Z_{rCl}^c (I_{rPV}^c - I_{rCC}^c - I_{rCP}^c) \end{bmatrix} \quad (13)$$

### 3.3. Calculation of system voltage

As discussed in the previous part, the currents of the line sections,  $[Iline]$ , are obtained through (7). Using the calculated currents together with the information of PVs and loads, the nodes voltages can be easily determined. (14) gets the voltage of an arbitrary phase ‘a’ node illustrated in Fig. 7. The calculated node voltages will be then used to update the values of the currents of PVs and constant power loads.

$$V_a = Z_{Cl}^a \left( I_{PV}^a + \sum_{i=1}^n I_i^a - I_{CC}^a - I_{CP}^a \right) \quad (14)$$

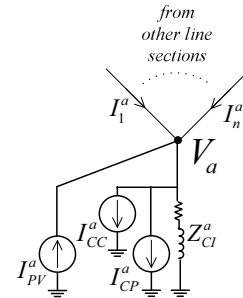


**Fig. 7.** Single-phase PV and loads connected to an arbitrary phase ‘a’ node.

### 3.4. Three-phase power flow

Fig. 8 shows the proposed algorithm for the power flow solution of a PV-dominated distribution network. As shown in the figure, the network solution, proposed in the previous part, calculates the state variables,  $[Iline]$ , from which the bus voltages are determined. The bus voltages are then passed to the models of PV and constant power load, introduced in section II, to update the values of the currents of PVs and constant power loads. This iteration runs until convergence is reached. Note that the characteristics of constant impedance and constant current loads do not need to be updated as they are represented with constant values in the network solution.

### 4. Test case

To evaluate the performance of the proposed method on a multiphase unbalanced distribution network, the IEEE 34 node test feeder is considered as the test case in this study. Since the original test feeder contains only radial sub-feeders, a number of lines were added to form it as a distribution network. Fig. 9 shows the modified test feeder. It's assumed that each customer has a PV system that can generate up to its maximum load of the customer unit (100% penetration).

The test case has been implemented using MATLAB to apply the proposed power flow solution. Figure 10 shows the sparsity pattern of the  $[Zbus]$  of the test case. As shown in the figure, the non-diagonal blocks are null matrices except the ones corresponding to interconnections. Therefore, the more interconnections a system has, the denser the  $[Zbus]$  will be.

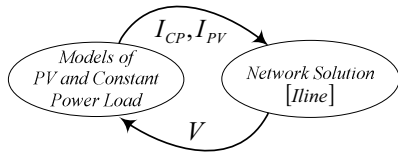


Fig. 8. Power flow solution for a multiphase unbalanced PV-dominated distribution network.

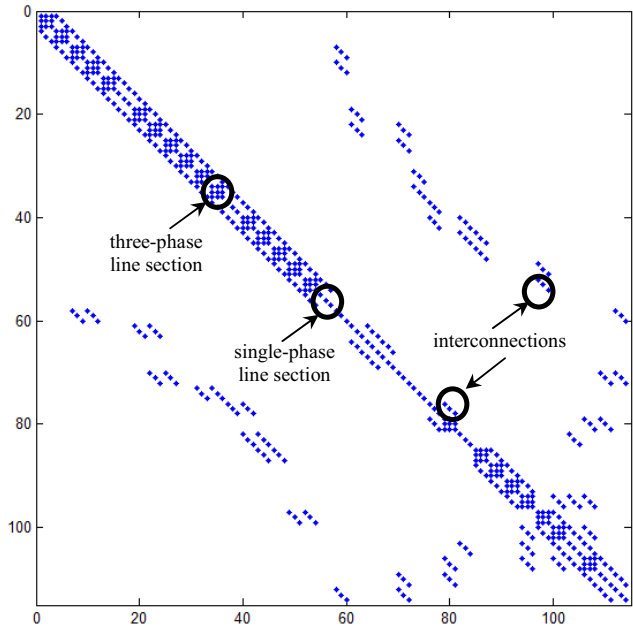


Fig. 10. Sparsity pattern of the  $[Zbus]$  of the test case.

In addition, the system is simulated using PSCAD in order to obtain detailed time domain simulations that are used for validating the proposed method. The PV system is simulated by adopting a typical model, which uses average models for the converters, and includes maximum power point tracker [12].

Tables I and II compare the results from the proposed methods with the results obtained from PSCAD simulations for a number of selected nodes (due to paper space limit). Simulation results were gathered after the initial transients damped. Results are obtained for two conditions: zero PV generation at night and maximum PV generation at noon. These results show that the solutions obtained from the proposed method are very close to the ones from PSCAD simulations. As indicated in the tables, the maximum differences between the results calculated by the proposed method and those obtained from the simulations for all nodes are less than 0.11% and 1.1% for the voltage magnitudes and the voltage angles, respectively.

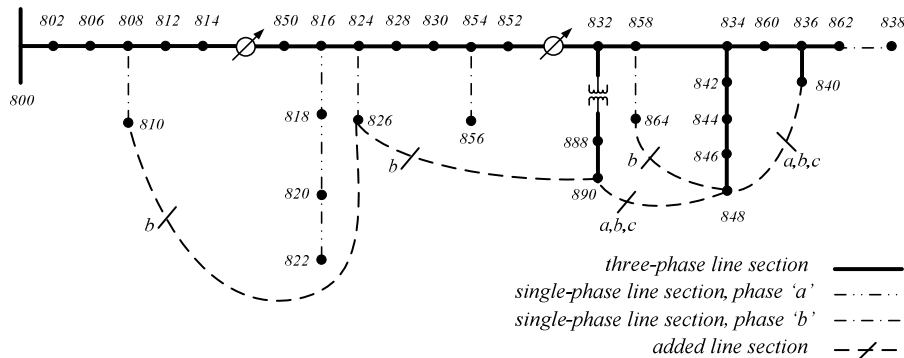


Fig. 9. Test case – Modified IEEE 34 node test feeder.

**Table 1.** Power flow results (No PV-Night)

Node	Phase	$ V _{p.u.}$ Simulation	$ V _{p.u.}$ Proposed Method	$<V$ deg. Simulation	$<V$ deg. (Proposed Method)
8	a	0.9974	0.9974	-0.0333	-0.0333
0	b	0.9976	0.9976	-120.0505	-120.0505
2	c	0.9978	0.9978	119.9542	119.9542
8	a	0.9127	0.9127	-0.8517	-0.8517
5	b	0.9569	0.9569	-120.2754	-120.2752
0	c	0.9217	0.9217	119.6644	119.6644
8	a	0.8618	0.8618	-0.9982	-0.9984
3	b	0.9327	0.9328	-119.9669	-119.9657
2	c	0.8503	0.8503	119.9584	119.9582
8	a	0.8615	0.8615	-1.0088	-1.009
9	b	0.9326	0.9326	-119.9717	-119.9705
0	c	0.8499	0.8499	119.9473	119.9472
8	a	0.8607	0.8607	-0.9947	-0.9969
6	b	0.9315	0.9315	-119.9604	-119.9592
2	c	0.8486	0.8486	119.946	119.9459
		Max. Dif. = 0.0118%		Max. Dif. = 0.2212%	

**Table 2.** Power flow results (Max PV-Noon)

Node	Phase	$ V _{p.u.}$ Simulation	$ V _{p.u.}$ Proposed Method	$<V$ deg. Simulation	$<V$ deg. (Proposed Method)
8	a	0.999	0.999	0.0647	0.0654
0	b	0.9989	0.9989	-119.9514	-119.9507
2	c	0.999	0.999	120.0501	120.0507
8	a	0.9698	0.9703	2.315	2.3344
5	b	0.9859	0.9862	-118.9488	-118.9406
0	c	0.9747	0.9752	122.1926	122.2038
8	a	0.9545	0.9554	3.8613	3.8888
3	b	0.9821	0.9825	-118.2101	-118.2003
2	c	0.958	0.959	124.484	124.5006
8	a	0.9543	0.9552	3.8695	3.8971
9	b	0.982	0.9824	-118.2075	-118.1977
0	c	0.9578	0.9588	124.4951	124.5118
8	a	0.9542	0.955	3.8982	3.9259
6	b	0.9818	0.9822	-118.1724	-118.1625
2	c	0.9575	0.9584	124.5343	124.5512
		Max. Dif. = 0.1044%		Max. Dif. = 1.0819%	

## 5. Conclusions

This paper proposed a new comprehensive power flow solution for multiphase unbalanced distribution networks with high penetration of PV systems. The proposed method considers the multiphase unbalanced systems as well as different system topologies. The method also considers the power flow contributions of PVs and different types of loads.

A modified IEEE 34 node test feeder was considered as the test case to evaluate the performance of the proposed method. The test feeder was simulated in PSCAD. The simulation based results were compared with those obtained from the proposed method. It was shown that the method provides quite accurate estimates.

Given that PV penetration on distribution level will increase in near future, the proposed method is much needed tool for a practicing engineer in assessing the impact of PV penetration on system operation and developing mitigating strategies.

## 6. Acknowledgement

H. Hooshyar and L. Vanfretti are supported by the FP7 IDE4L project funded by the European Commission.

L. Vanfretti is supported by Statnett SF, the Norwegian transmission system operator, and the STandUP for Energy Collaboration Initiative.

## 7. References

- [1] J. Teng, "A direct approach for distribution system load flow solutions", *IEEE Trans. Power Del.*, vol. 18, no. 3, pp. 882-887, Jul., 2003.
- [2] S. Khushalani, N. Schulz, "Unbalanced distribution power flow with distributed generation", in *IEEE PES Transmission and Distribution Conference and Exhibition*, 2006, pp. 301-306.
- [3] M. E. Baran, H. Hooshyar, Z. Shen, A. Huang, "Accommodating high PV penetration on distribution feeders", *IEEE Trans. Smart Grid*, vol. 3, no. 2, pp. 1039-1046, Jun., 2012.
- [4] L. Zhang, Y. Zhao, S. Wang, W. Tang, "A novel hybrid power flow algorithm for distribution system with DGs", in *Asia-Pacific Power and Energy Engineering Conference (APPEEC)*, 2010, pp. 1-5.
- [5] J. Teng, "Integration of distributed generators into distribution three-phase load flow analysis", in *IEEE Power Tech*, 2005, pp. 1-6.
- [6] F.J. Ruiz-Rodriguez, J.C. Hernández, F. Jurado, "Probabilistic load flow for radial distribution networks with photovoltaic generators", *IET Journal on Renewable Power Generation*, vol. 6, no. 2, pp. 110-121, Mar., 2012.
- [7] Syafii, K.M. Nor, M. Abdel-Akher, "Analysis of three phase distribution networks with distributed generation", in *IEEE 2nd International Power and Energy Conference (PECon)*, 2008, pp. 1563-1568.
- [8] Syafii, K.M. Nor, M. Abdel-Akher, "Grid-connected Photovoltaic models for three-phase load flow analysis", in *IEEE International Power and Energy Conference (PECon)*, 2010, pp. 544-548.
- [9] M.Z. Kamh, R. Iravani, "Unbalanced model and power-flow analysis of microgrids and active distribution systems", *IEEE Trans. Power Del.*, vol. 25, no. 4, pp. 2851-2858, Oct., 2010.
- [10] IEEE P1547.7™/D4.0, "Draft Guide to Conducting Distribution Impact Studies for Distributed Resource Interconnection".
- [11] H. Hooshyar, M. E. Baran, "Fault analysis on distribution feeders with high penetration of PV systems", *IEEE Trans. Power Sys.*, vol. 28, no. 3, pp. 2890-2896, Aug., 2013.
- [12] Model available on the website of ECEE department at the University of Colorado at Boulder (<http://ecee.colorado.edu/~ecen2060/matlab.html>).